https://doi.org/10.5194/egusphere-2026-6703
Preprint. Discussion started: 11 November 2026
© Author(s) 2026. CC BY 4.0 License.

Crop Flood Risk in the United States: Linking Flood Frequency, Duration, and Crop-Specific Damage

Md. Asif Rahman[1], Eric Tate[2], Sina Razzaghi Asl[3], Miguel Diaz Garcia[4], Antonio Arenas[4]

[1]California Governor's Office of Emergency Services, Sacramento, 95655, USA
[2]Center for Research on Energy and the Environment, Princeton University, Princeton, 08540, USA
[3]Department of Political Science and Geography, Old Dominion University, Norfolk, 23529, USA
[4]Department of Civil Construction and Environmental Engineering, Iowa State University, Ames, 50011, USA

Correspondence to: Eric Tate (eric.tate@princeton.edu)

Abstract. Crops in the coterminous United States are highly exposed to inland floods, yet large-scale estimates of crop-specific flood losses remain limited. Existing assessments are often geographically constrained and rely on a coarse empirical understanding of the relationship between flood duration and crop damage. To address these gaps, we developed a new nationwide library of frequency-duration-damage functions and applied it to determine the magnitude and spatial distribution of crop flood loss. The damage functions were empirically constructed by combining streamflow-based frequency-duration analysis with crop-specific duration–damage relationships from satellite-derived vegetation indices. We implemented the resulting functions in the HEC-FIA flood loss model, along with geospatial data on riverine and pluvial flood hazard, crop distribution, and crop production, to estimate economic losses for six major crops at watershed and state scales. Total annualized loss is approximately USD 258 million for a baseline June 1 flood scenario, with losses concentrated in the Upper Mississippi River Basin. Corn and soybeans account for over 85% of total loss, while alfalfa, non-alfalfa hay, cotton, and rice experience smaller but regionally significant impacts. Relative loss patterns differ from absolute losses, with the highest proportional losses occurring in the Appalachian Valley, New England, and parts of the West. This study provides the first known national-scale assessment of crop-specific flood losses that integrates flood frequency-duration-damage relationships, enabling the identification of priority regions and crops for targeted adaptation. Future work should refine empirical frequency-duration-damage relationships and assess the sensitivity of crop loss estimates to model assumptions.

Keywords: crop flood risk, flood duration, crop damage, average annualized loss, duration-damage functions

https://doi.org/10.5194/egusphere-2026-6703
Preprint. Discussion started: 11 November 2026
© Author(s) 2026. CC BY 4.0 License.

1 Introduction

Inland floods cause substantial crop loss in the United States, and many major crop-producing regions are flood-prone (Rahman & Di, 2020). High-damage floods occurred near the Mid-Atlantic coast in 2011 (Suro et al., 2015), in the Upper Mississippi River basin in 2011 (Di et al., 2017), and in the Missouri River basin in 2019 (Huffstutter & Pamuk, 2019; Reed et al., 2020). Floods reduce crop yield and are significant drivers of large crop insurance payments (ClimateAi, 2020; Yildirim & Demir, 2022). Climate change-driven increases in flood frequency, magnitude, intensity, and duration are extending production disruptions, with cascading and compounding effects across the entire food supply chain (Bolster et al., 2023). Such impacts heighten the importance of reliably quantifying the severity and distribution of crop flood risk.

Crop flood loss assessments occur throughout the disaster cycle, but large-scale pre-disaster studies of US crop flood losses are rare. Indeed, post-disaster assessment is the most common and tends to analyze long-term and indirect impacts to inform insurance payments, federal assistance, and flood mitigation planning (Di et al., 2017; Shan et al., 2010; Tapia-Silva et al., 2011). Loss assessment during disasters can help delineate the real-time extent of flood impacts (Brémond et al., 2013), determine emergency support needs, and inform modeling of future flood loss estimates (Merz et al., 2010). Pre-disaster assessments identify areas with high loss potential, which can help develop mitigation plans (Bhakta Shrestha et al., 2019), inform crop insurance policies (Di et al., 2017), and guide crop selection and planting times (Citeau, 2003). Conducting pre-disaster spatial loss assessments across a large geographic area would improve understanding of crop flood risk and provide a foundation for enhancing flood mitigation measures.

Although flood duration is a primary determinant of crop damage and yield loss (Förster et al., 2008; Shrestha et al., 2017), existing crop-loss models seldom link duration to flood frequency. Soil oxygen and nitrogen decrease during inundation, adversely affecting root health, plant height, leaf area and greenness, disease resistance, and mortality (Kaur et al., 2020). Crops inundated for one or two days may survive with only minimal damage or yield loss, but as flood duration increases, so does the likelihood and severity of damage. Flood duration is also related to flood frequency, with longer durations generally associated with lower frequencies. To account for varying flood frequencies, Maroof (2016) used the HAZUS flood loss estimation model to evaluate 3-, 4-, 7-, and 14-day flood durations and assigned associated crop damage modifiers. Similarly, Yildirim & Demir (2022) examined 1-, 3-, and 7-day flood durations across seasonal contexts, but assumed a total crop loss for each event. Neither study linked flood durations with flood frequencies, a practice emblematic of current US crop loss analyses that treat flood duration as fixed rather than frequency-dependent. While flood risk modeling for buildings is facilitated by a wealth of structure-specific depth-damage functions, a principal obstacle to large-scale crop risk analysis is the absence of crop-specific duration-frequency-damage functions.

Crop flood vulnerability depends on crop-specific, geographic, and flood-duration factors that existing models underrepresent. While some research has explored duration-damage dynamics in other countries (e.g., Monteleone et al., 2023; Bhakta Shrestha et al., 2019), comparable studies in the US are virtually nonexistent. Empirical studies that incorporate geographically varying duration-damage relationships are exceedingly rare. Other influential contextual factors include the extent and duration of the flood event (Bhakta Shrestha et al., 2019), crop location and

https://doi.org/10.5194/egusphere-2026-6703
Preprint. Discussion started: 11 November 2026
© Author(s) 2026. CC BY 4.0 License.

type (Förster et al., 2008), planting and harvesting dates (Penning-Rowsell & Wilson, 2003), planting cost (Dutta et al., 2003), sale price (Ahmed et al., 2017), and yield (Brémond et al., 2013). Yet crop flood risk analyses (predictive or modeled) rarely capture the full range of input parameters that influence loss.

The few existing large-scale US crop risk assessments diverge in their flood loss estimates. FEMA's National Risk Index models annualized crop flood losses at the national scale using flood exposure, crop locations, county-level crop values, and historical loss ratios (FEMA, 2023). They reported an average annualized loss (AAL) of USD 386 million from flooding. The analysis was spatially distributed but did not disaggregate losses by crop type, consider crop-specific production value, or model the variable relationships among flood exposure, duration, and crop damage (FEMA, 2023; Zuzak et al., 2022). At the state level, Yildirim & Demir (2022) used eight flood return periods to model riverine AAL for corn, soybean, sweet corn, and alfalfa in Iowa in the HAZUS Flood Model. They calculated a total AAL of USD 230 million.

Collectively, existing research on flood crop loss leaves three important gaps unaddressed: assessing pre-disaster economic risk at large scales, linking flood duration and flood frequency in spatially explicit analysis, and employing crop-specific duration-damage relationships. This study addresses these deficiencies by quantifying direct crop flood loss in the coterminous US (CONUS). The analysis is organized around the following research questions:

1. What is the relationship between flood frequency, flood duration, and crop damage?
2. What is the crop flood risk in the CONUS, and how does it vary across crops and geographies?

To investigate, we conducted hydrologic and remote sensing analyses to develop a new set of regionally varying crop loss functions that link flood duration, return period, and crop-specific damage. The functions were applied in a flood loss model, alongside nationwide spatial data on flood extent and crop distributions, and state-level information on planting costs and harvest yields.

2 Data and Methods

We estimated flood risk by combining flood exposure, flood frequency-duration analysis, crop-specific duration-damage relationships, state-specific crop production characteristics, and HEC-FIA modeling (Fig. 1). Flood frequency-duration estimates were derived from historical streamflow data using a peaks-over-threshold method, and we subsequently established crop-specific duration–damage relationships by analyzing percentage changes in the Vegetation Condition Index (VCI). We linked the two to create a state-specific library of flood frequency-duration-damage functions for crops in the CONUS. Combined with inputs of flood extent, crop locations, terrain elevations, and measures of crop production, the damage functions were a central input to flood risk estimation using the HEC-FIA model.

https://doi.org/10.5194/egusphere-2026-6703
Preprint. Discussion started: 11 November 2026
© Author(s) 2026. CC BY 4.0 License.

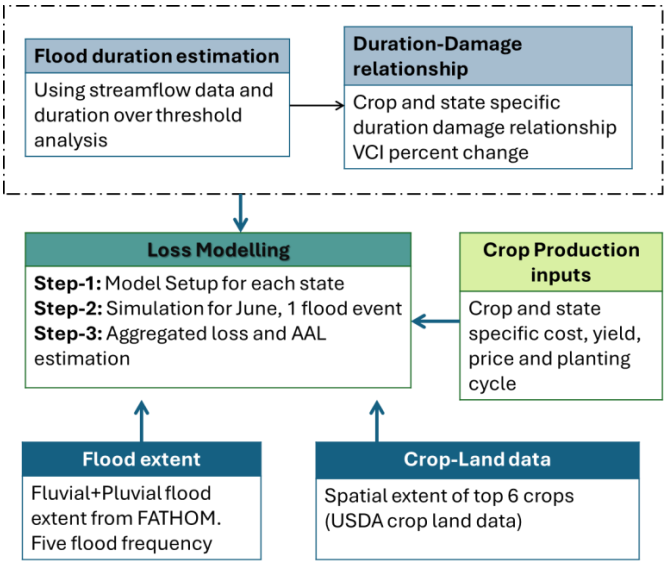


Figure 1: Crop Loss Analysis Framework.

2.1 Flood Duration

To estimate the flood duration in gaged locations, we implemented a novel duration-over-threshold (DOT) model. It identifies consecutive periods during which discharge exceeds a specified threshold, estimates their frequency, and maps the resulting durations across CONUS. The methodology is based on flood frequency analysis, considering statistical approaches proposed in prior studies (Dawdy et al., 2012; England et al., 2018; Feng et al., 2017), and automated by Lawson et al. (2025). To deploy the model, we retrieved CONUS streamflow data from the National Water Information System (NWIS, 1998) at 15- to 60-minute intervals, based on data available in records. The flow data are based on instantaneous values reported for gages by the US Geological Survey (USGS), from 1986 to 2024. The model evaluates flood events based on the duration of flows that exceed defined thresholds in the time-series data. This yields peaks-over-threshold data to develop a relationship between threshold discharge and the derived set of flood durations (Lawson et al., 2025). The thresholds were computed using flows that produced mean arrival rates of two events per year for the peak-over-threshold computation (Lawson et al., 2025). After generating the peaks-over-threshold data, the model fits a Pareto-Poisson distribution with a convenient similarity to a Generalized Extreme Value type statistical distribution and a power-law regression to estimate the arrival rate (Lawson et al., 2025). The DOT model accounts for all the overland flow over the basin's catchment. For example, during extreme rain (e.g., Cedar River, Iowa in 2008), the data capture both riverine and pluvial effects.

To establish the flood event duration as how often the flow exceeds a threshold for a given q for at least d days, using the arrival rate estimates from the statistical model, plots for each one of the evaluated gages were computed, extracting the intersection of arrival rate curves for each recurrence with the flow threshold for a 2-year recurrence, considering this flow as the terminal point for the flooding events.

https://doi.org/10.5194/egusphere-2026-6703
Preprint. Discussion started: 11 November 2026
© Author(s) 2026. CC BY 4.0 License.

We focused on seven Annual Exceedance Probabilities (AEPs) for the duration over threshold model: 20%, 10%, 4%, 2%, 1%, 0.5%, and 0.2%, which correspond to recurrence intervals of 5, 10, 25, 50, 100, 200, and 500 years, respectively. We retrieved AEP flow values from Stream Stats (USGS, 2019) and extracted historical flow and basin polygons from the Hydro Network-Linked Data Index and the USGS National Water Information System using the data-retrieval Python package developed by Hodson et al. (2023). Using these calculations, we generated gridded values for each recurrence interval with an inverse-weighted conservative distance interpolation method, as typically applied in flood mapping analysis (Villa & Gianinetto, 2006; Zarekarizi et al., 2021). From the gridded data, spatial mean values for the number of consecutive hours at each recurrence interval were estimated for the CONUS to determine trends in flood susceptibility based on historical streamflow data. For example, Fig. 2 shows the DOT model outputs for the Little Calumet River at Porter, Indiana (USGS Gage 04094000), which has a similar duration range to historical events such as the 2008 event reported in Porter, Indiana (Fowler et al., 2010).

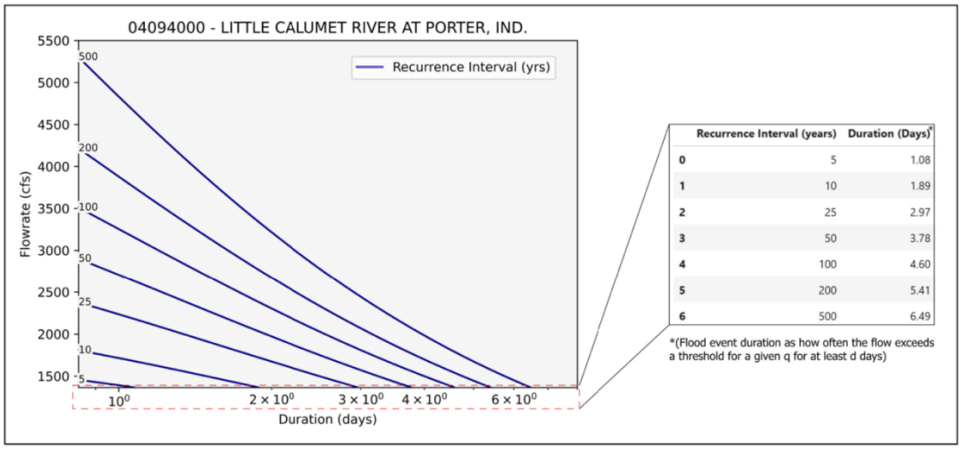


Figure 2: Flood duration based on a 2-year recurrence terminal flow threshold for recurrences of 5 to 500 years return periods at USGS Gage 04094000 location.

Figure 3 presents the spatial distribution of flood duration for the 0.2% annual-exceedance-probability event, based on DOT estimates. Black triangles identify the USGS gage data used in the analysis, while the shaded watersheds represent estimated consecutive flood durations in days ranging from approximately 1 to 14 days.

https://doi.org/10.5194/egusphere-2026-6703
Preprint. Discussion started: 11 November 2026
© Author(s) 2026. CC BY 4.0 License.

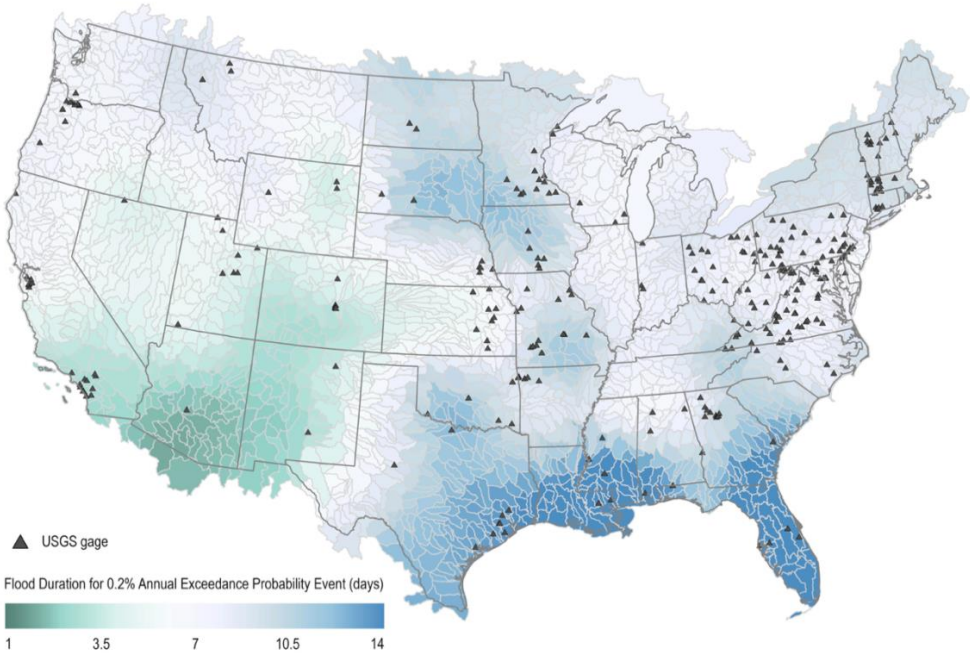


Figure 3: Spatial distribution of consecutive flood duration in the USA for 0.2% annual exceedance probability event calculated using arrival rates from the peaks-over-threshold DOT model.

2.2 Duration damage functions

We developed duration-damage-frequency (DDF) functions and curves to estimate crop-specific flood-induced damage across different flood frequencies for multiple U.S. states. We began the analysis by importing flood duration data by return period and assembling a table of percent change in a vegetation condition index for six major crops (Corn, Soybeans, Alfalfa, Non-Alfalfa, Cotton, and Rice) across five representative flood durations based on remotely sensed satellite data.

2.2.1 Crop condition profile analysis

We evaluated crop damage by analyzing vegetation indices before and after flood events and by comparing current crop conditions against historical baselines (Rahman et al., 2021). We then characterized spatial variability in planted crops and flood impacts using the Cropland Data Layer (CDL) and Landsat imagery. The CDL is a 30-meter-resolution gridded dataset that describes crop locations and other land cover types, such as forests, shrubland, permanent water bodies, wetlands, idle land, and developed regions. We downloaded the 2008, 2011, and 2017 CDL datasets from the USDA National Agricultural Statistics Service (NASS) and reclassified them based on the six crop types. Landsat 8 and 7 satellite imagery from USGS was used to analyze vegetation conditions before and after each flood event within a two-week window, capturing the effects on crop damage. We used 30-meter Sentinel-1 Synthetic Aperture Radar imagery from NASA Disaster Mapping to identify flood boundaries during multiple

https://doi.org/10.5194/egusphere-2026-6703
Preprint. Discussion started: 11 November 2026
© Author(s) 2026. CC BY 4.0 License.

events. We then matched flood event data with satellite imagery, CDL crop distributions, and geospatial extents to align datasets across regions, crop types, and temporal windows.

The analysis covered flood durations of 3, 4, 6, 8, and 12 days, corresponding to significant flood events. We defined a significant flood event as a riverine flood that satisfied three criteria:

(1) had cloud-tolerable Landsat 7/8 coverage within the two-week pre- and post-flood window required for the VCI comparison, in or adjacent to a CDL reference year (2008, 2011, 2017)
(2) reached NOAA billion-dollar disaster status or triggered a FEMA disaster declaration
(3) inundated a substantial extent of cropland in one or more of the six target crop classes, as confirmed by Sentinel-1 SAR flood boundaries overlaid on the CDL

Applying these criteria yielded five flood events: the Flint watershed along the Mississippi River, Iowa (May 29-June 10, 2008); the lower Wabash watershed, Indiana (June 7-9, 2008); the Lower Mississippi watershed, Missouri (May 3-10, 2011); the Missouri River near Blair-Omaha, Nebraska (June 27-July 1, 2011); and the Black River, Arkansas (May 1-4, 2017).

The crop condition profile analysis focused on the Vegetation Condition Index (VCI), which proxies vegetation greenness and vigor and serves as an indicator of chlorophyll and moisture content (Liu & Kogan, 1996). VCI values range from 0 to 100, with lower values indicating poor vegetation health (e.g., drought-like conditions) and higher values indicating optimal conditions. The VCI was calculated using Eq. 1, based on the Normalized Difference Vegetation Index (NDVI):

$$VCI = (NDVI - NDVI_{min})/(NDVI_{max} - NDVI_{min}) \times 100 \quad (1)$$

Where $NDVI_{min}$ and $NDVI_{max}$ represent the historical minimum and maximum NDVI values for a specific location and period, providing a baseline for evaluating vegetation conditions. NDVI is calculated using Eq. 2.

$$NDVI = (NIR - RED)/(NIR + RED) \quad (2)$$

NIR represents the reflectance in the near-infrared band, and RED represents the reflectance in the red band. For each of the six crops, the percentage change in VCI was calculated using Eq. 3:

$$\%\Delta VCI = (VCI_{after} - VCI_{before})/(VCI_{before}) \times 100 \quad (3)$$

Where VCI_{after} is the post-flood VCI value, and VCI_{before} is the pre-flood VCI value. By calculating the percentage change in VCI for each crop, we assessed the flood's impact on vegetation damage across different inundation durations (Table 1). The spatial and computational analyses were conducted in ArcGIS Pro and using the **raster, sf**, **dplyr**, and **tidyverse** packages in R 4.3.0.

https://doi.org/10.5194/egusphere-2026-6703
Preprint. Discussion started: 11 November 2026
© Author(s) 2026. CC BY 4.0 License.

Table 1. Change in VCI by crop type and flood duration based on specific flood events.

Crop type	% VCI change by Flood Duration (days)					Lag time (days)
	3	4	6	8	12	
Corn	17.91	19.08	23.67	28.50	66.09	5
Soybeans	18.00	21.00	27.00	36.00	54.00	6
Alfalfa	5.76	8.76	12.36	15.30	27.51	4
Non-alfalfa hay	6.39	21.54	26.52	36.69	55.35	6
Cotton	5.25	9.00	16.50	24.00	39.00	5
Rice	3.00	6.00	12.00	18.00	30.00	7

To account for delayed vegetation responses to flooding, we determined lag periods for each crop based on the phenological literature. The lag time in Table 1 represents the delay between the onset of flood inundation and the time at which damage becomes evident in vegetation reflectance data. This delay occurs because physiological stress from waterlogging, such as root hypoxia, nutrient deficiency, or leaf chlorosis, takes time to manifest visually and be detected by satellite-derived indices (e.g., NDVI or VCI). For example, corn typically shows visible stress within 2–4 days of flooding, with NDVI reductions detectable within 3–5 days (Shrestha et al., 2017). Rice exhibits a slower response, particularly in less flood-tolerant varieties, with symptoms and reflectance changes emerging after 5 days (Juraimi et al., 2009).

We used SAR imagery to delineate floodplain extents because major flood events typically coincide with persistent cloud cover. This limits the availability of optical imagery during times of peak inundation. SAR operates independently of cloud cover and illumination and detects open water through its low backscatter, making it well suited to capturing flood extent while water remains on the landscape. Optical Landsat imagery was then used to assess vegetation condition before and after each event, for which multispectral reflectance is better suited. The two imagery sources thus played complementary roles: SAR identified where flooding occurred, and Landsat-derived VCI measured the crop response.

2.2.2 Frequency-duration-damage function

We estimated VCI percent changes at non-observed durations using piecewise linear interpolation between the five calibration durations (3, 4, 6, 8, and 12 days), preserving the nonlinear acceleration in crop damage observed at longer inundation durations. We then incorporated crop-specific lag times representing delayed physiological responses to flooding, which were added to each flood duration. The lag durations shown in Table 1 were extracted from the literature (Scott et al., 1989; Linkemer et al., 1998; Bange et al., 2004; Wang et al., 2017). Finally, we merged the interpolated VCI damage estimates with flood durations for each crop and return period, producing a combined dataset reflecting expected percent damage for each crop type by state and flood frequency.

https://doi.org/10.5194/egusphere-2026-6703
Preprint. Discussion started: 11 November 2026
© Author(s) 2026. CC BY 4.0 License.

2.3 HEC-FIA modeling inputs

2.3.1 Geospatial data

Table 2 shows the HEC-FIA geospatial data inputs, their description, and sources. All data were preprocessed in ArcGIS Pro before input into HEC-FIA. HEC-FIA requires Digital Elevation Model (DEM) data covering the study area to create a watershed configuration, a prerequisite for setting the model's flood extent, arrival, and duration parameters. We downloaded DEM data from the National Map, a USGS geospatial data portal (USGS, 2022). The elevation data are stored in 1° × 1° tiles (~110 × 110 km^2), and 1,011 tiles cover CONUS. We downloaded the tiles and mosaicked them in ArcGIS to create the DEM dataset.

Table 2. Geospatial input data for HEC-FIA.

Data	Description	Source
DEM	1/3 arc second digital elevation model for CONUS	USGS
Crop distribution	National crop land data (crop extent and type)	Cropland Data Layer (CDL) from National Agricultural Statistical Services (NASS)
Flood extent	10 m fluvial and pluvial flood grid (extent and depth) for CONUS	FATHOM-US flood model v2.0
Project boundary	Shapefile for each state	US Census
Arrival grid	Time of flood arrival	Prepared from flood depth grid data
Duration grid	Duration of the flood event (based on flood frequency and time)	Prepared using streamflow data and flood frequency analysis (see section 2.1)

We derived spatially explicit crop information from the 2021 CDL (USDA-NASS, 2022), a georeferenced, crop-specific raster layer of land cover. The CDL is generated from satellite imagery and is the only available dataset that provides annual, crop-specific locations at the national scale (Lark et al., 2021). The CDL spatial accuracy is good for major crops and locations but is less adept at capturing locations for some other crops and land cover (e.g., alfalfa hay, grassland) (Lark et al., 2021; L. Lin et al., 2022). We selected the top six field crops in the US by total acreage in the CDL: corn, soybean, cotton, rice, alfalfa, and non-alfalfa hay. One or more of these dominate the total cropped area in almost every state. Selecting these crops excludes prominent crops in some states but also enables a detailed duration-damage assessment.

We analyzed flood risk using five flood return periods for the CONUS: 5, 50, 100, 200, and 500 years, accounting for high- and low-frequency floods. The GIS flood depth grids were obtained from FATHOM to represent flood hazard at a spatial resolution of 10 meters. For each return period, the grids model both fluvial (riverine) and pluvial (surface water) hazards (FATHOM, 2021). We removed permanent water bodies (e.g., rivers and lakes) from each grid cell, then mosaicked the fluvial and pluvial datasets and classified all cells with a depth greater than zero as wet.

https://doi.org/10.5194/egusphere-2026-6703
Preprint. Discussion started: 11 November 2026
© Author(s) 2026. CC BY 4.0 License.

The FATHOM methodology has been validated and applied in numerous flood-related studies (Bates et al., 2021; Tate et al., 2021; Wing et al., 2018, 2022). Refer to Wing et al. (2017, 2018) for a more detailed description of the flood grids.

We then prepared the HEC-FIA duration and arrival grids using the areal extent of the mosaicked grids. The arrival time grid represents the time at which flooding reaches a predefined depth threshold in each cell. The recommended threshold for crop assessment in HEC-FIA is 0 feet, so we created a raster grid with a constant value of 0 to serve as the arrival grid. The duration grid represents the time that each grid cell is inundated. Based on the analysis results in Section 2.1, we created a duration raster for each flood frequency and state.

2.3.2 Crop production data

Crop production attributes are important modeling parameters but vary significantly across crops and states. We extracted crop-specific production information (Table 3) from both NASS and agricultural extension offices at state land-grant universities. The variables in Table 3 are based on 2022, except for planting and harvest times. The most recently updated information on planting and harvest times was available in a 2010 NASS publication (USDA 2010).

Table 3. Crop production input data for HEC-FIA.

Data	Description	Source
Fixed cost	Monthly fixed cost of planting	State agricultural extension offices
Variable cost	Monthly variable cost of planting	
Harvest cost	Cost of harvest	
Yield	Crop yield per acre	NASS
Price	Crop price per unit	
Planting date	Start date for 1st & 2nd planting	
Harvest date	Date of harvest date	

To collect crop parameter values for each state, we visited the crop production cost information webpage and downloaded the latest year's data. However, each state provides data in different time frames, and some states have missing variables. Missing variables were more common in the smaller states on the East Coast (e.g., Vermont, New Hampshire, Rhode Island, Delaware, and Massachusetts). We also had difficulty finding data for nonalfalfa hay in some states. To address missing information, we used the average of available data from neighboring states. To account for variability in time and yield, we adjusted costs to 2022 and used NASS yield values. HEC-FIA requires monthly fixed and variable planting costs for each crop, but that information is only available as a total cost. Therefore, we equally distributed the total cost across the months from planting to harvest.

https://doi.org/10.5194/egusphere-2026-6703
Preprint. Discussion started: 11 November 2026
© Author(s) 2026. CC BY 4.0 License.

2.4 Model calculations

We selected five flood return periods as the basis for the risk analysis in each state: 10, 50, 100, 200, and 500 years. The selection is based on our flood-duration estimates and the nationwide flood-depth grid from FATHOM. In the model for each state, most of the input data remain constant except the flood grid, flood arrival grid, flood duration grid, and simulation start and end times. The duration-damage relationship for each crop and state was assigned based on the previously described methodology.

We selected a June 1 scenario as the baseline flood timing to reflect the primary flood season of much of the Corn Belt, where a high degree of crop flood exposure lies. Flooding is common here after winter snowmelt and can be amplified by heavy rainfall in late May and early June. Heavy snowfall the preceding winter, waterlogged soils, and high-intensity spring rains are a classic precursor to major floods in the main crop-producing belt of the Upper Mississippi River basin. We also selected a June 1 flood scenario to assess the impact of loss savings from a potential second planting of crops following flooding. Large-scale flooding certainly occurs at other times of the year, and selecting different flood simulation dates would generate different loss values, especially when flooding occurs near planting or harvest. However, analyzing multiple flood dates is beyond the scope of this study.

The crop loss calculation primarily depends on two factors. The first is the value added by the farmer to the field at the time of flooding, meaning the amount of the crop's economic value that is in the field on the first day of flooding. This is derived from the crop's fixed and variable costs, its stage in the planting cycle, and its potential yield and price. The second factor is the relationship between flood duration and crop damage. This means a crop's damage depends on flood duration and its timing within the planting season.

The initial output of each model run is the total economic loss at each crop location. The spatial unit for these values is the raster cell (30 x 30 m), each representing a specific crop location. During the analysis, HEC-FIA converts each crop raster cell into a point at its centroid, with an associated output of dollar loss and flooded acreage. We aggregated the point-loss data for each crop to two spatial scales: (1) Hydrological Unit Code-8 (HUC8) boundaries, because flooding occurs at the watershed scale, and (2) the state level.

AAL is a standard metric for modeling future flood loss for hazard mitigation. It is the expected annual economic loss that would occur if the financial losses from all potential flood hazards, weighted by their expected probabilities, were spread equally over time (Armal et al., 2020; Gnan et al., 2022). Essentially, AAL is the frequency-weighted economic loss across return periods. One key aspect of AAL estimation is selecting the number of return periods to include in the calculation. Messner et al. (2007) suggest using six different return periods for a proper estimation. AAL is more sensitive to higher-frequency floods, so oversampling is needed when damage could increase drastically (Tate et al., 2016; Ward et al., 2011). In quantifying crop losses in Iowa, Yildirim and Demir (2022) used eight return periods (2, 5, 10, 25, 50, 100, 200, and 500 years). We used losses from five return periods (10, 50, 100, 200, and 500 years) from the FATHOM dataset to compute AAL with Eq. 4:

$$AAL = (P_{10} - P_{50})\left(\frac{L_{10}+L_{50}}{2}\right) + (P_{50} - P_{100})\left(\frac{L_{50}+L_{100}}{2}\right) + (P_{100} - P_{200})\left(\frac{L_{100}+L_{200}}{2}\right) + (P_{200} - P_{500})\left(\frac{L_{200}+L_{500}}{2}\right) + P_{500}L_{500} \quad (4)$$

where P is the flood frequency, and L is the associated crop loss.

https://doi.org/10.5194/egusphere-2026-6703
Preprint. Discussion started: 11 November 2026
© Author(s) 2026. CC BY 4.0 License.

3 Results

This section summarizes the results of our three research questions. This includes a summary of the flood frequency and duration calculation, the relationship between flood duration and crop damage, the total AAL for the top six major crops in the US, and the distribution of losses by crop and geography.

3.1 Flood frequency-duration and duration-damage relationships

Research question 1 focuses on the empirical relationship between flood frequency, flood duration, and crop damage. We begin with frequency-duration. Figure 2 maps recurrent threshold exceedances for the 500-year flood event, particularly along the Eastern and Southeastern seaboards and in portions of the Midwest. Building on these estimates, Fig. 4 shows the average annual flood duration for each state across multiple return periods. Florida has the longest mean flood durations for most frequencies, while Arizona consistently has the shortest. Other states with historically high flood impacts (Iowa, Illinois, Louisiana, Mississippi, Texas, Arkansas) also demonstrate comparatively long flood durations. These patterns reflect the abundance of flood events in these areas, along with their flat topography and slow-moving water systems (Marti et al., 2023). A complete listing of mean flood-duration values by state and flood frequency is provided in Supplementary Table 1.

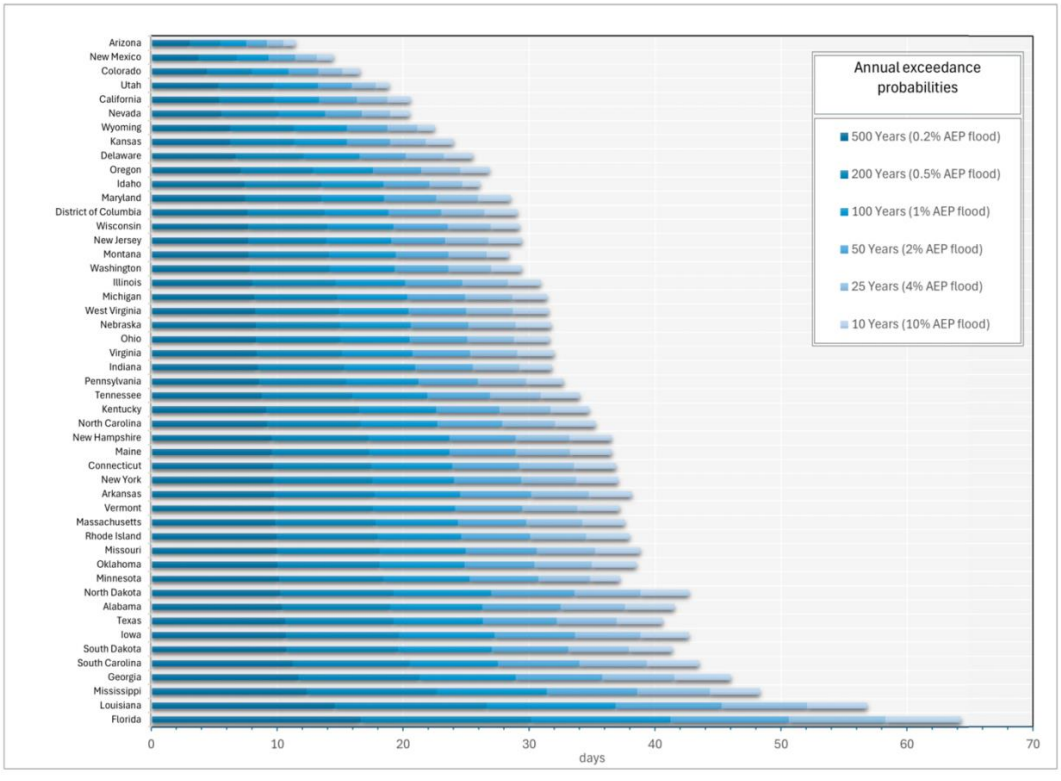


Figure 4: Average flood duration for each annual exceedance probability by state.

https://doi.org/10.5194/egusphere-2026-6703
Preprint. Discussion started: 11 November 2026
© Author(s) 2026. CC BY 4.0 License.

We identified the duration-damage relationship for each crop in each state, based on changes in crop profiles and their relationship to flood duration. Figure 5 shows the flood duration damage curve for the top six crops in the US, and Fig. 6 shows their flood frequency-duration-damage curves (provided numerically in Supplemental Table 2). Corn has the highest percentage change in damage, followed by non-alfalfa hay and soybeans, while rice has the smallest. For a given duration, damage is higher in New England, Florida, North Dakota, South Dakota, and Western states.

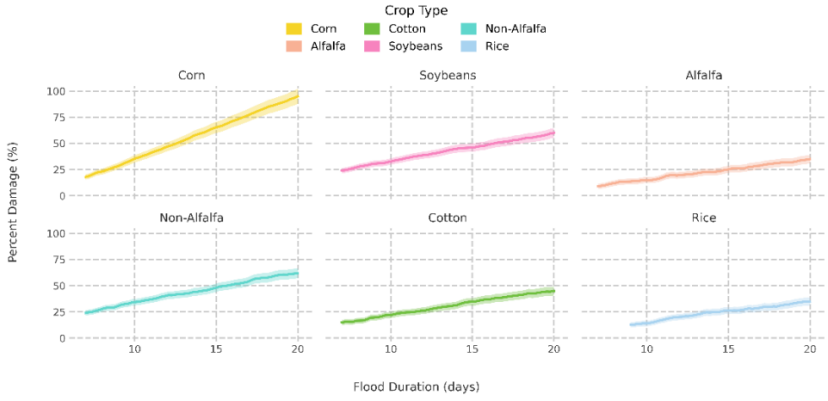


Figure 5: Flood duration-damage curves for six crop types in the U.S.

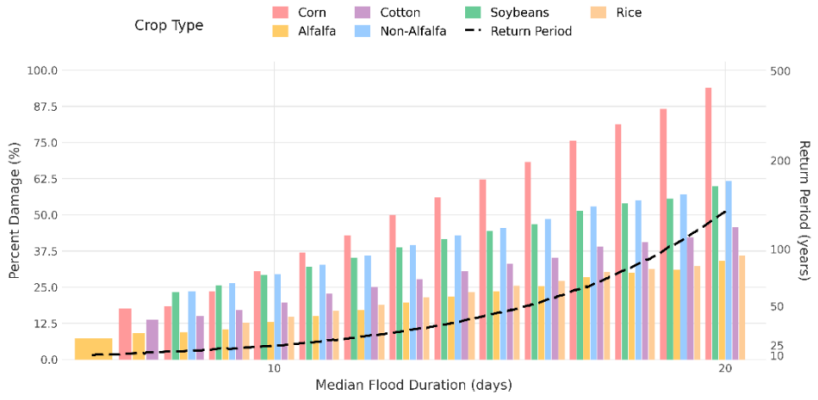


Figure 6: Flood frequency-duration-damage curves for six crop types in the U.S.

3.2 Total AAL

Research question 2 examines crop flood risk and its geographic and crop-specific distributions. Across the top six crops in the CONUS, the total AAL is approximately USD 258 million for the June 1 flood simulation. Figure 7(a) shows the AAL distribution at the HUC8 watershed scale. The light-to-dark green color scheme represents AAL from low to high, including watersheds with no loss (i.e., no intersection between flood extent and crop location) in

https://doi.org/10.5194/egusphere-2026-6703
Preprint. Discussion started: 11 November 2026
© Author(s) 2026. CC BY 4.0 License.

parts of Nevada and Arizona. Flood AAL is relatively more concentrated in the high-crop-producing regions of the Midwest and the lower Mississippi River basin, as well as Idaho, California, North Dakota, Kansas, and the Appalachian Valley.

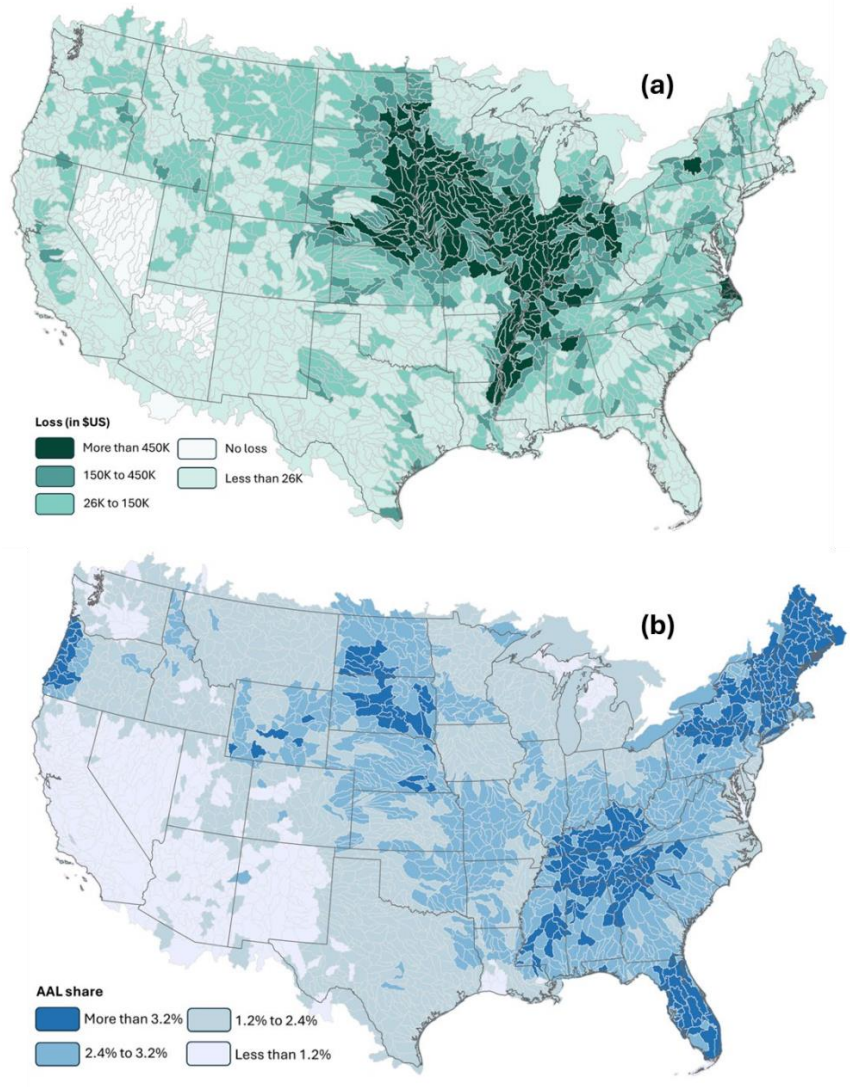


Figure 7: HUC-8 scale distributions of (a) total AAL and (b) AAL share as a percentage of total crop value.

Absolute AAL (Fig. 7a) and relative AAL normalized by the total crop value (Fig. 7b) have distinct spatial patterns as they measure different dimensions of economic loss. The highest relative AAL (approx. 3.2% or more) predominates in the Appalachian Valley, New England, Oregon, Florida, and North Dakota and South Dakota, while relative AAL is approximately 2.4% to 3.2% in the Midwest and Mississippi River basins. Both the degree of crop flood exposure in each state and the variability in crop value contribute to the divergence between absolute and relative loss. Higher

https://doi.org/10.5194/egusphere-2026-6703
Preprint. Discussion started: 11 November 2026
© Author(s) 2026. CC BY 4.0 License.

absolute AAL mostly correlates with high crop production and high flood inundation. By contrast, relative loss can be higher in places with comparatively lower crop production activity and flood exposure. Because the geography of high relative loss identifies places where a large share of available crops is lost, it is a potentially better indicator of regional economic impact than absolute loss.

A few states dominate the geography of the absolute AAL. For comparison, Fig. 8 shows the top 10 states by AAL and their 100-year floodplain exposure. The blue bar shows each state's total AAL, and the orange line indicates the total inundated crop area. Heavy crop-producing states in the US Midwest have the highest total AAL. Illinois (IL) has the highest value at about USD 35 million, while Iowa (IA) is USD 28 million. Nebraska (NE) ranks next with USD 25 million, while Minnesota (MN) and Indiana (IN) have nearly USD 18 million. The other top-10 states are Missouri (MO), South Dakota (SD), Ohio (OH), Kansas (KS), and Kentucky (KY).

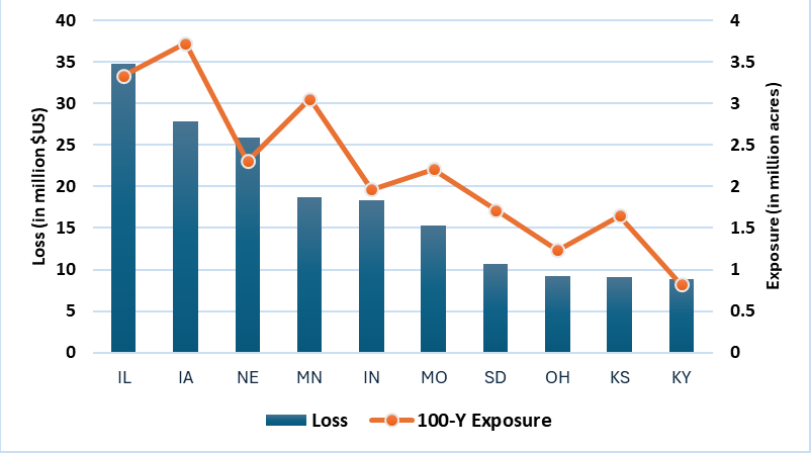


Figure 8: Highest AAL states and the associated inundated crop area for the 100-year flood.

Crop value has a strong impact on the spatial distribution of overall loss. By rank of total inundated area, Iowa has a lower total AAL than Illinois despite higher crop exposure. The average crop value is the combination of crop production costs, yield, price, and planting seasonality. Similarly, Minnesota has more exposed crop area than Nebraska, but a lower AAL. Kansas has higher flood exposure than Ohio despite having a similar AAL. Crop value is even lower in Minnesota, reflected in lower AAL despite higher exposure.

3.3 Crop-specific AAL

Per-acre crop value varies substantially across states and is a source of divergence between flood exposure and economic loss. Figure 9 shows the per-acre crop value of corn and soybean for the nine states with the highest AAL. The crop value is the sum of resources invested in the field at a given time and over the crop-production season. Illinois has the highest corn value, followed by Iowa, Nebraska, Missouri, and Ohio. Among the top states, South Dakota had the lowest per-acre value for corn on June 1. Soybean values are higher in Illinois, Indiana, and Iowa, while Minnesota has the lowest value on the list.

https://doi.org/10.5194/egusphere-2026-6703
Preprint. Discussion started: 11 November 2026
© Author(s) 2026. CC BY 4.0 License.

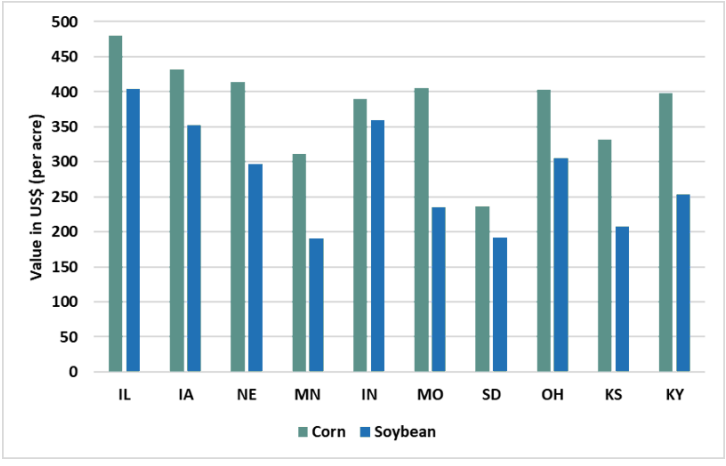


Figure 9: Crop value per acre on June 1.

Figure 10 shows the top six crops and their total AAL. Corn has the highest total loss at USD 131.9 million, while soybeans total USD 93.4 million. Alfalfa and nonalfalfa hay have losses of USD 10.8 and 15.7 million, respectively, while cotton's estimated loss is USD million.

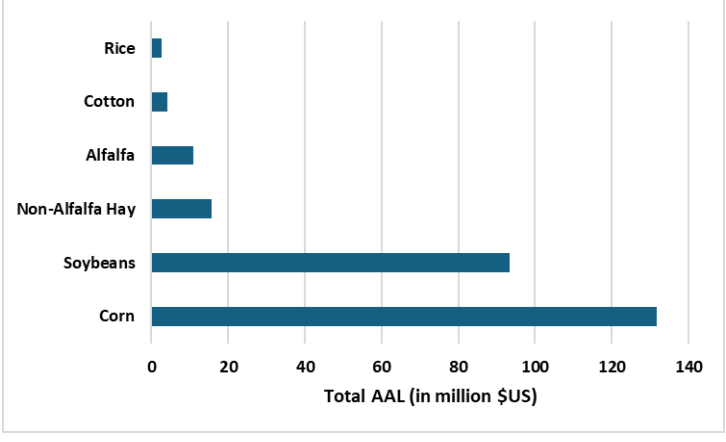


Figure 10: AAL for major crops.

Figure 11 shows the spatial distribution of AAL for the six highest-loss crops. The crops with the highest AAL are corn and soybeans. For corn, the highest AAL is in the Midwest and the Mississippi River basin, at more than USD 400,000 per watershed. Corn also has high losses in North Dakota, South Dakota, and Virginia.

https://doi.org/10.5194/egusphere-2026-6703
Preprint. Discussion started: 11 November 2026
© Author(s) 2026. CC BY 4.0 License.

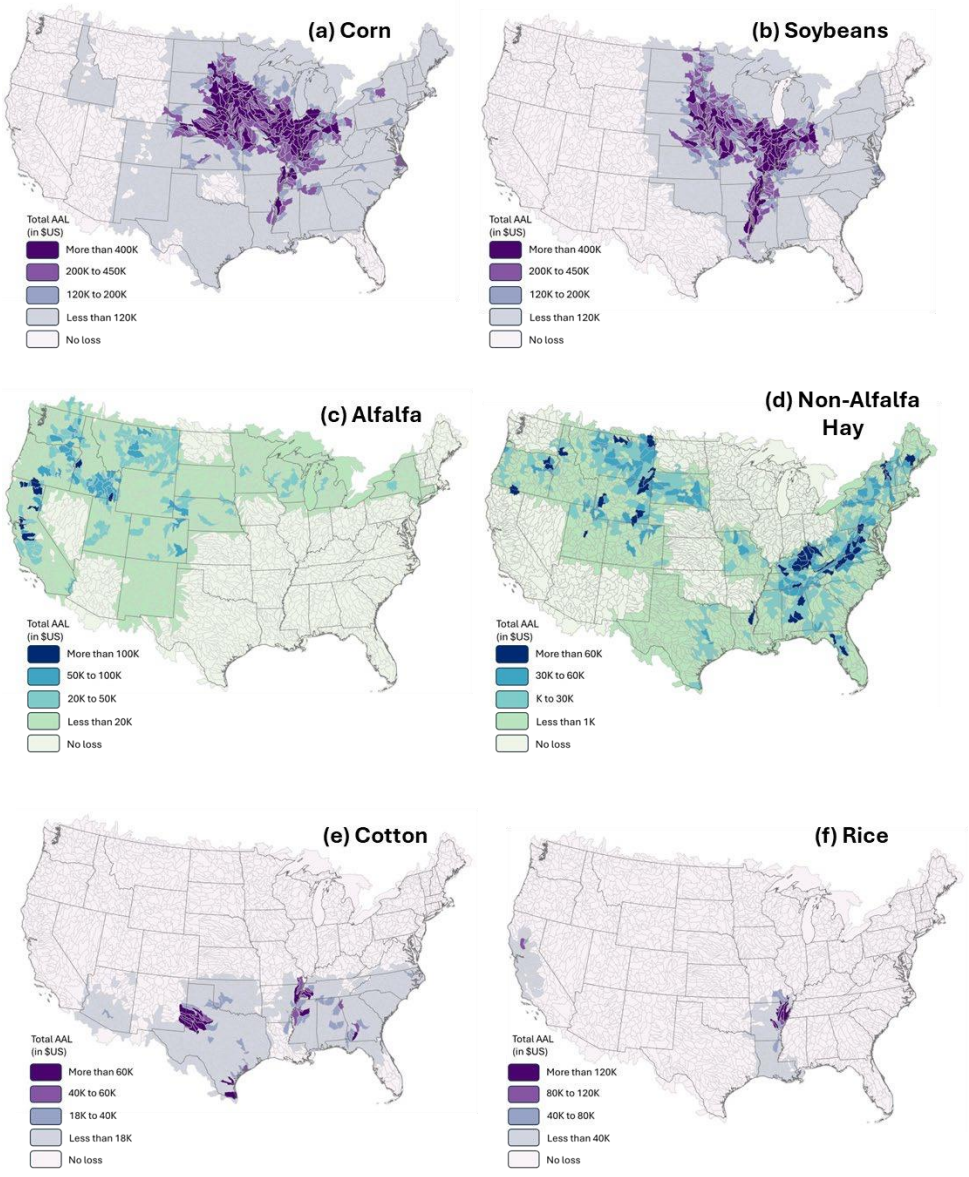


Figure 11: AAL distribution for the six crops with the highest losses.

Soybean AAL follows a similar distribution, mainly concentrating in the Midwest and Lower Mississippi Basin. The highest estimated soybean loss exceeds USD 400,000 per watershed. The AAL distribution for hay follows a different pattern than that for corn and soybeans. For alfalfa, losses are higher in western US watersheds. This region's AAL exceeds USD 100,000 per watershed. The second classification in Fig. 10(c), the USD 50,000-100,000 range, is also dominant in the West. Higher AAL occurs in the Northern Plains, Southeast, and Appalachian Valley for non-alfalfa hay. The higher concentration of non-alfalfa hay loss also coincides with the geography of

https://doi.org/10.5194/egusphere-2026-6703
Preprint. Discussion started: 11 November 2026
© Author(s) 2026. CC BY 4.0 License.

relative loss, suggesting potentially greater flooding impacts. The highest AAL exceeds USD 60,000 per watershed. Cotton and rice are not produced in most states. For cotton, higher losses are primarily concentrated in the Lower Mississippi River Basin and Texas. For rice, the high-loss areas are Arkansas, Louisiana, and California.

4 Discussion

Our results offer a new understanding of the relationships among flood duration, frequency, and damage; the spatial distribution of crop loss; the agreement among crop risk estimates; and what is needed to improve crop flood-risk modeling. Along with cropping strategies for flood adaptation, we discuss these below.

4.1 Comparison of crop risk estimates

Our estimate of absolute AAL across major crops in CONUS is USD 258 million. By contrast, the National Risk Index quantified the total AAL for crops from flooding at USD 386 million (FEMA, 2023). The reasons for the divergence could very well be methodological. The National Risk Index uses the county-level average crop value and historical flood events to calculate its loss ratio. By contrast, we applied a HEC-FIA model that included flood hazard, state-specific crop and planting data, June 1 flood timing, and duration-damage functions that vary with flood frequency. The substantial differences in modeling approaches challenge a clean comparison of loss estimates.

US crop insurance indemnity payments provide another point of comparison. As flood frequency and severity have increased in the US, insurance payments for flooded cropland have skyrocketed. According to an assessment by the Environmental Working Group, insurance payments for crop losses from flooding and drought have tripled since 1995 (Yale Environment 360, 2022). Total insurance payments under the excess moisture/precipitation peril category (which includes flooding) were USD 38 billion between 1995 and 2021 (EWG, 2022; Schechinger, 2022). This equates to an average of USD 1.45 billion per year. However, the excess moisture peril includes heavy rainfall, saturated soils, and standing water, and pays out for both inhibited planting and yield loss. Our AAL estimate is based on a much narrower set of loss drivers: crop damage from flood hazard.

Factors other than flooding could also explain the difference between loss estimates and insurance payments. For example, our AAL results are based on modeling for the single year 2022, but crop production attributes, such as production cost, yield, and price, can vary substantially from year to year. This variability influences the exposed crop value. Floods occurring at other times of the year, such as the August or September harvesting season, may generate greater losses because they affect more of the crop's value. This could over- or underestimate AAL, potentially further contributing to the differences in insurance payments.

4.2 Absolute vs. relative risk

The geography of crop flood risk differs substantially depending on whether risk is measured in terms of absolute or relative loss. Absolute flood risk is highest in the Midwest and the Mississippi River basin, where the majority of planted acreage is corn and soybeans. Elsewhere, substantial losses occur for alfalfa, nonalfalfa hay, cotton, and rice. Outside the farm belt, comparatively higher AAL coincides with the crop-producing regions of California, Idaho,

https://doi.org/10.5194/egusphere-2026-6703
Preprint. Discussion started: 11 November 2026
© Author(s) 2026. CC BY 4.0 License.

and the Appalachian region. The magnitude of loss in these places reflects higher crop value and a higher percentage of inundated crop area, with Illinois and Iowa having the highest AAL. By contrast, relative loss is highest in the Appalachian Valley, New England, and Idaho. Crop loss in these places may place greater strain on farmers and communities, positioning relative loss as a potentially stronger indicator of regional economic impact.

4.3 Adaptation strategies

Areas with higher losses can be ideal priority locations for implementing adaptation actions. These may include restoring riparian vegetation, adopting flood-tolerant crop varieties (Kaur et al., 2020), shifting planting and harvest dates (Kaur et al., 2020; Kucharik, 2006), planting cover crops, and improving drainage (Blanco-Canqui et al., 2015). Planting flood-tolerant crop varieties in flood-exposed areas can reduce losses during longer-duration floods. Most crops have a specific planting window for each season. Using this and potential flooding information, shifting the planting season by starting later or harvesting earlier may reduce flood impacts. Analyses in Iowa have found that planting cover crops during the dormant winter season in high-flood-impact areas can reduce flood impacts (Basche et al., 2016; Antolini et al., 2020).

Some of the highest flood-exposed places can be converted into conservation areas and retired from crop production. The USDA Agricultural Conservation Easement Program is designed to create partnerships with farmland owners and conserve them as functional wetlands. Spatially distributed flood loss estimates can help prioritize selecting land for such an effort. For example, in the Mississippi River Critical Conservation Area (MRCCA), there have been USD 1.5 billion in flood-related crop insurance payments that could be used for large-scale conservation (Gustin, 2022). Identifying watersheds with higher potential flood losses is a potentially critical step in floodplain conservation (Karwowski, 2022), as it can reduce insurance payments at the expense of tax dollars. If loss information is coupled with soil quality and crop suitability, it can be used to identify areas for retirement and conservation.

The salience of diversification as a flood adaptation strategy is likely to increase as climate change amplifies hydrologic impacts. For example, farmers can adopt alternative production methods and rotate crops to address seasonal flooding (Chonabayashi et al., 2020; Lin, 2011). Cultivating diverse crops with varying flood tolerance can offset damage to a single crop (Birthal & Hazrana, 2019). Despite its benefits, diversification faces several economic and institutional barriers, including limited market access, extensive commercialization of crop production (Weisberger et al., 2021), and low motivation among some farmers to diversify due to weather-related events (Roesch-McNally et al., 2018).

Adaptation strategies adopted in one high-risk watershed for a given crop might be shared and implemented in locations with similar loss levels. Many farmers also traditionally rely upon recent memories of flood incidents to decide whether to plant (Mase et al., 2017; Reyes & Elias, 2019; Steele et al., 2018). Estimating flood loss and identifying high-risk areas can be effective tools for reducing cognitive bias in agricultural decision-making.

https://doi.org/10.5194/egusphere-2026-6703
Preprint. Discussion started: 11 November 2026
© Author(s) 2026. CC BY 4.0 License.

4.4 Future modeling needs

Advance development of frequency-duration-damage functions. The relationship between flood frequency, flood duration, and crop damage is vastly underexplored in empirical studies, and is both geographically and temporally nonstationary. Indeed, prior research has identified a global trend toward more frequent moderate-duration floods in the subtropics and long-duration floods in the midlatitudes (Najibi and Devineni, 2018). While there are established depth-damage functions for analyzing building flood risk, there is a general absence of established duration-damage functions suitable for crop risk analysis. We thus calibrated the duration-damage functions using five river flood events in Iowa, Indiana, Nebraska, Missouri, and Arkansas. However, applying these functions to climatically and pedologically distinct regions, including cotton in Texas, rice in California, and alfalfa in the arid West, assumes that VCI-based crop responses to inundation duration are transferable across geographic contexts. Factors limiting transferability include differences in soil drainage, antecedent moisture, cultivar selection, and irrigation practices. Loss estimates for regions outside the Midwest calibration domain therefore carry higher uncertainty. Empirical calibration using more flood events, particularly in other regions, is a priority for future work.

Standardize crop production reporting across crops and states. The crop production data we employed included variable and fixed production costs, planting timeline, harvest cost and time, crop price, and yield. HEC-FIA uses these factors to compute the estimated crop value at a given time in the planting cycle. Using such a breadth of production factors not only generates a more accurate representation of crop value but could also identify which crop characteristics most influence modeled flood loss. The loss estimation could be further enhanced by modeling crop attributes across different years to assess their effects on AAL. However, the ability to do this is constrained by a lack of uniformity in the availability of crop production information across states and time. Although NASS collects annual data on crop prices and yields, information on crop production costs, harvest costs, and planting cycles is available only in some states. Data availability is higher in the major crop-producing states, particularly for corn, soybean, rice, and cotton. There is a need to standardize attribute reporting across crops and states to enable more accurate estimation of crop value at each time of year. Land-grant universities, typically the primary source of crop production cost information, could take the initiative to develop a universal data format.

Perform sensitivity analyses. Further studies are needed to assess how output loss estimates vary with input modeling parameters, including flood duration, flood timing, crop types, crop production, harvest cost, variability in the planting cycle, and analysis scale. Doing so would enable a more robust understanding of how floods affect crop loss. Temporally, we modeled a June 1 flood to reflect the late-spring timing of major past floods in the Corn Belt region where loss totals are greatest. But because crop value generally increases over the growing season, June 1 simulations overshoot losses from early-season floods and undershoot those from late-season floods (Antolini et al., 2020). As such, our AAL estimate of USD 258 million likely reflects a median crop-loss scenario. Simulating additional flood dates would enhance understanding of the relationship between flood timing and flood loss.

Uncertainties in the remote sensing inputs also warrant further evaluation. Although SAR-derived flood boundaries are unaffected by cloud cover, SAR can underestimate inundation over emergent crops, where double-bounce scattering produces bright rather than dark returns. Cross-validation against independent optical water maps would help quantify this effect.

https://doi.org/10.5194/egusphere-2026-6703
Preprint. Discussion started: 11 November 2026
© Author(s) 2026. CC BY 4.0 License.

Our analysis focused on the six most prevalent crops based on the CDL. Expanding the modeling to include additional crops, such as winter wheat, canola, sorghum, and sugarcane, would enhance the comprehensiveness and accuracy of crop flood-loss estimates. Spatially, we aggregated the loss totals by HUC8 watershed boundaries. The point-level computations in HEC-FIA also allow losses to be aggregated to other spatial scales, such as census tracts, counties, and states. Finally, by applying projected future crop prices, locations, and flood hazard, modeling could predict future losses, providing scientific information relevant for crop adaptation decision-making.

5 Conclusions

Flood loss assessments for crops in the US are few, limited in geographic scope, and rely on coarse empirical relationships between flood duration and crop damage. This study advances prior research by conducting the first nationwide flood risk assessment for crops in the coterminous US, based on frequency-duration-damage functions and state-specific cropping characteristics. By combining hydrologic analysis of flood frequency and duration with remote sensing-based analysis of duration and crop damage, we created a library of frequency-duration-damage functions for six crops. Applying the functions in HEC-FIA to characteristics of crops exposed to riverine and pluvial flooding produced an average annual loss of USD 258 million for a baseline scenario on June 1.

Mapping the multiple dimensions of loss at the watershed scale identified divergence in disaggregated flood risk. Absolute loss is highest in the Mississippi River basin and is dominated by corn and soybeans. By contrast, relative loss is highest in the Appalachian Valley, New England, Florida, Oregon coast, and the Dakotas. Thus, the relationship between flood frequency, duration, and damage varies with both crop type and geography. The loss estimates and damage functions provide information that can support agricultural adaptation, floodplain conservation, crop insurance evaluation, and prioritization of flood mitigation investments. Future work should strengthen frequency-duration-damage functions through analysis of additional flood events, and quantify losses for more crops and different points in the growing season.

Code and data availability

An online Zenodo archive (doi.org/10.5281/zenodo.23751157) includes three elements:

1. Supplementary Table 1, containing mean flood-duration values by state and flood frequency.
2. Supplementary Table 2, containing state-specific frequency-duration-damage relationships for all six crops.
3. The R script used to construct the Vegetation Condition Index (VCI)-based damage estimation.

All data used in this study are publicly available from the sources cited in the main text. The flood loss analyses were performed using HEC-FIA, which is available from the Hydrologic Engineering Center of the US Army Corps of Engineers (https://www.hec.usace.army.mil/software/hec-fia/). All other calculations were carried out using standard software.

https://doi.org/10.5194/egusphere-2026-6703
Preprint. Discussion started: 11 November 2026
© Author(s) 2026. CC BY 4.0 License.



Author contributions

MAR - Conceptualization, Methodology, Formal analysis, Visualization, Writing - Original Draft; **ET** - Conceptualization, Methodology, Writing - Review & Editing; **SRA** - Methodology, Formal analysis, Visualization, Writing - Review & Editing; **MDG** - Conceptualization, Data curation, Investigation, Methodology, Software, Validation, Visualization, Writing – Review & Editing; **AA** - Methodology, Writing - Review & Editing

Competing interests

The authors declare that they have no conflict of interest.

Disclaimer

Copernicus Publications remains neutral with regard to jurisdictional claims made in the text, published maps, institutional affiliations, or any other geographical representation in this paper. While Copernicus Publications makes every effort to include appropriate place names, the final responsibility lies with the authors. Views expressed in the text are those of the authors and do not necessarily reflect the views of the publisher.

Financial contributions

None.

References

Ahmed, M. R., Rahaman, K. R., Kok, A., & Hassan, Q. K. (2017). Remote Sensing-Based Quantification of the Impact of Flash Flooding on the Rice Production: A Case Study over Northeastern Bangladesh. *Sensors*, *17*(10), 2347. https://doi.org/10.3390/s17102347.

Antolini, F., Tate, E., Dalzell, B., Young, N., Johnson, K., & Hawthorne, P. L. (2020). Flood risk reduction from agricultural best management practices. *JAWRA Journal of the American Water Resources Association*, *56*(1), 161-179. https://doi.org/10.1111/1752-1688.12812.

Armal, S., Porter, J. R., Lingle, B., Chu, Z., Marston, M. L., & Wing, O. E. J. (2020). Assessing property level economic impacts of climate in the US, new insights and evidence from a comprehensive flood risk assessment tool. *Climate*, *8*(10), 116. https://doi.org/10.3390/cli8100116.

Bange, M. P., Milroy, S. P., & Thongbai, P. (2004). Growth and yield of cotton in response to waterlogging. *Field crops research*, *88*(2-3), 129-142. https://doi.org/10.1016/j.fcr.2003.12.002.

Basche, A. D., Kaspar, T. C., Archontoulis, S. V, Jaynes, D. B., Sauer, T. J., Parkin, T. B., & Miguez, F. E. (2016). Soil water improvements with the long-term use of a winter rye cover crop. *Agricultural Water Management*, *172*, 40–50. https://doi.org/10.1016/j.agwat.2016.04.006.

https://doi.org/10.5194/egusphere-2026-6703
Preprint. Discussion started: 11 November 2026
© Author(s) 2026. CC BY 4.0 License.



Bates, P. D. , Quinn, N. , Sampson, C. , Smith, A. , Wing, O. , Sosa, J. , et al. (2021). Combined modeling of US fluvial, pluvial, and coastal flood hazard under current and future climates. *Water Resources Research*, *57*(2), e2020WR028673. https://doi.org/10.1029/2020WR028673.

Bhakta Shrestha, B., Sawano, H., Ohara, M., Yamazaki, Y., & Tokunaga, Y. (2019). Methodology for Agricultural Flood Damage Assessment. In *Recent Advances in Flood Risk Management*. IntechOpen. https://doi.org/10.5772/intechopen.81011/.

Birthal, P. S., & Hazrana, J. (2019). Crop diversification and resilience of agriculture to climatic shocks: Evidence from India. *Agricultural Systems*, *173*, 345–354. https://doi.org/10.1016/j.agsy.2019.03.005.

Blanco-Canqui, H., Shaver, T. M., Lindquist, J. L., Shapiro, C. A., Elmore, R. W., Francis, C. A., & Hergert, G. W. (2015). Cover Crops and Ecosystem Services: Insights from Studies in Temperate Soils. *Agronomy Journal*, *107*(6), 2449–2474. https://doi.org/10.2134/agronj15.0086.

Bolster, C.H., R. Mitchell, A. Kitts, A. Campbell, M. Cosh, T.L. Farrigan, A.J. Franzluebbers, D.L. Hoover, V.L. Jin, D.E. Peck, M.R. Schmer, and M.D. Smith, 2023: Ch. 11. Agriculture, food systems, and rural communities. In: Fifth National Climate Assessment. Crimmins, A.R., C.W. Avery, D.R. Easterling, K.E. Kunkel, B.C. Stewart, and T.K. Maycock, Eds. U.S. Global Change Research Program, Washington, DC, USA. https://doi.org/10.7930/NCA5.2023.CH11/.

Brémond, P., Grelot, F., & Agenais, A.-L. (2013). Review Article: Economic evaluation of flood damage to agriculture – review and analysis of existing methods. *Natural Hazards and Earth System Sciences*, *13*(10), 2493–2512. https://doi.org/10.5194/nhess-13-2493-2013.

Chonabayashi, S., Jithitikulchai, T., & Qu, Y. (2020). Does agricultural diversification build economic resilience to drought and flood? Evidence from poor households in Zambia. *African Journal of Agricultural and Resource Economics*, *15*(311-2020–1781), 65–80. https://doi.org/10.22004/ag.econ.307618.

Citeau, J. M. (2003). A new control concept in the Oise catchment area: definition and assessment of flood compatible agricultural activities. *FIG Working Week, Paris, France*, *19*.

ClimateAi. (2020). *The Impact of Floods on Agriculture in the U.S. — Taking a Look Under the Hood*. ClimateAi. https://climateai.medium.com/the-impact-of-floods-on-agriculture-in-the-u-s- taking-a-look-under-the-hood-5b3d3ddf307e.

Dawdy, D. R., Griffis, V. W., & Gupta, V. K. (2012). Regional Flood-Frequency Analysis: How We Got Here and Where We Are Going. *Journal of Hydrologic Engineering*, *17*(9), 953–959. https://doi.org/10.1061/(ASCE)HE.1943-5584.0000584.

Di, L., Yu, E. G., Kang, L., Shrestha, R., & BAI, Y. (2017). RF-CLASS: A remote-sensing-based flood crop loss assessment cyber-service system for supporting crop statistics and insurance decision-making. *Journal of Integrative Agriculture*, *16*(2), 408–423. https://doi.org/10.1016/S2095-3119(16)61499-5.

https://doi.org/10.5194/egusphere-2026-6703
Preprint. Discussion started: 11 November 2026
© Author(s) 2026. CC BY 4.0 License.



Dutta, D., Herath, S., & Musiake, K. (2003). A mathematical model for flood loss estimation. *Journal of Hydrology*, *277*(1–2), 24–49. https://doi.org/10.1016/S0022-1694(03)00084-2.

England Jr, J.F., Cohn, T.A., Faber, B.A., Stedinger, J.R., Thomas Jr, W.O., Veilleux, A.G., Kiang, J.E. and Mason Jr, R.R. (2018). *Guidelines for determining flood flow frequency — Bulletin 17C*. https://doi.org/10.3133/tm4B5.

EWG. (2022). *Crop Insurance in the United States*. Environmental Working Group. https://farm.ewg.org/cropinsurance.php?fips=00000&regionname=theUnitedStates.

FATHOM. (2021). *Fathom-US 2.0*. https://www.fathom.global/fathom-us

FEMA. (2023). *The National Risk Index*. https://hazards.fema.gov/nri/.

Feng, Y., Brubaker, K. L., & McCuen, R. H. (2017). New View of Flood Frequency Incorporating Duration. *Journal of Hydrologic Engineering*, *22*(11), 04017051. https://doi.org/10.1061/(ASCE)HE.1943-5584.0001573.

Förster, S., Kuhlmann, B., Lindenschmidt, K. E., & Bronstert, A. (2008). Assessing flood risk for a rural detention area. *Natural Hazards and Earth System Sciences*, *8*(2), 311-322. https://doi.org/10.5194/nhess-8-311-2008.

Fowler, K. K., Kim, M. H., Menke, C. D., & Arvin, D. V. (2010). *Flood of September 2008 in Northwestern Indiana*.

Gnan, E., Friedland, C. J., Rahim, M. A., Mostafiz, R. Bin, Rohli, R. V, Orooji, F., Taghinezhad, A., & McElwee, J. (2022). Improved building-specific flood risk assessment and implications of depth-damage function selection. *Frontiers in Water*, *4*, 919726. https://doi.org/10.3389/frwa.2022.919726.

Gustin, G. (2022, March 30). *US Taxpayers Are Spending Billions on Crop Insurance Premiums to Prop Up Farmers on Frequently Flooded, Unproductive Land*. Inside Climate News. https://insideclimatenews.org/news/30032022/crop-insurance-premiums-flood-agriculture/.

Hodson, T. O., & Hariharan, J. A. (2023). dataretrieval (python): a Python package for discovering and retrieving water data available from Federal hydrologic web services. *US Geological Survey (USGS) Software*, 50. https://doi.org/10.5066/P94I5TX3.

Huffstutter, P., & Pamuk, H. (2019). *Exclusive: More than 1 million acres of U.S. cropland ravaged by floods*. Reuters. https://www.reuters.com/article/us-usa-weather-floods-exclusive- idUSKCN1RA2AW.

Juraimi, A. S., Saiful, M., Begum, M., Anuar, A. R., & Azmi, M. (2009). Influence of flooding intensity and duration on rice growth and yield. *Pertanika J. Trop. Agric. Sci*, *32*(2), 195-208.

Karwowski, N. (2022). *Estimating the Effect of Easements on Agricultural Production*. National Bureau of Economic Research.

Kaur, G., Singh, G., Motavalli, P. P., Nelson, K. A., Orlowski, J. M., & Golden, B. R. (2020). Impacts and management strategies for crop production in waterlogged or flooded soils: A review. *Agronomy Journal*, *112*(3), 1475–1501. https://doi.org/10.1002/agj2.20093.

Kucharik, C. J. (2006). A Multidecadal Trend of Earlier Corn Planting in the Central USA. *Agronomy Journal*, *98*(6), 1544–1550. https://doi.org/10.2134/agronj2006.0156.

https://doi.org/10.5194/egusphere-2026-6703
Preprint. Discussion started: 11 November 2026
© Author(s) 2026. CC BY 4.0 License.

Lark, T. J., Schelly, I. H., & Gibbs, H. K. (2021). Accuracy, bias, and improvements in mapping crops and cropland across the United States using the USDA Cropland Data Layer. *Remote Sensing*, *13*(5), 968. https://doi.org/10.3390/rs13050968.

Lawson, K. S., Underwood, K. L., Diehl, R. M., & Rizzo, D. M. (2025). A Duration-Over-Threshold Model for Flood Frequency and Flow Regime Characterization. *Water Resources Research*, *61*(2). https://doi.org/10.1029/2023WR037022.

Lin, B. B. (2011). Resilience in Agriculture through Crop Diversification: Adaptive Management for Environmental Change. *BioScience*, *61*(3), 183–193. https://doi.org/10.1525/bio.2011.61.3.4.

Lin, L., Di, L., Zhang, C., Guo, L., Di, Y., Li, H., & Yang, A. (2022). Validation and refinement of cropland data layer using a spatial-temporal decision tree algorithm. *Scientific Data*, *9*(1), 63. https://doi.org/10.1038/s41597-022-01169-w.

Linkemer, G., Board, J. E., & Musgrave, M. E. (1998). Waterlogging effects on growth and yield components in late-planted soybean. *Crop Science*, *38*(6), 1576-1584. https://doi.org/10.2135/cropsci1998.0011183X003800060028x.

Liu, W. T., & Kogan, F. N. (1996). Monitoring regional drought using the vegetation condition index. *International Journal of Remote Sensing*, *17*(14), 2761-2782. https://doi.org/10.1080/01431169608949106.

Maroof, M. A. S. (2016). *Assessing the influence of parameters for agricultural flood loss estimation in the Middle Cedar River Watershed, Iowa* (pp. x, 73 pages). University of Iowa.

Marti, M. K., Ryberg, K. R., & Levin, S. B. (2023). Flood-frequency analysis in the Midwest: Addressing potential nonstationarity of annual peak-flow records. *AASHTO Hydrolink*, (22), 9- 11.

Mase, A. S., Gramig, B. M., & Prokopy, L. S. (2017). Climate change beliefs, risk perceptions, and adaptation behavior among Midwestern U.S. crop farmers. *Climate Risk Management*, *15*, 8–17. https://doi.org/10.1016/j.crm.2016.11.004.

Merz, B., Kreibich, H., Schwarze, R., & Thieken, A. (2010). Review article "assessment of economic flood damage." *Natural Hazards and Earth System Science*, *10*(8), 1697–1724. https://doi.org/10.5194/nhess-10-1697-2010.

Messner, F., Penning-Rowsell, E., Green, C., Meyer, V., Tunstall, S., & van der Veen, A. (2007).

Evaluating flood damages: guidance and recommendations on principles and methods.

Monteleone, B., Giusti, R., Magnini, A., Arosio, M., Domeneghetti, A., Borzì, I., Petruccelli, N., Castellarin, A., Bonaccorso, B., & Martina, M. L. V. (2023). Estimations of Crop Losses Due to Flood Using Multiple Sources of Information and Models: The Case Study of the Panaro River. *Water*, *15*(11), 1980. https://doi.org/10.3390/w15111980.

Najibi, N., & Devineni, N. (2018). Recent trends in the frequency and duration of global floods. *Earth System Dynamics*, *9*(2), 757–783. https://doi.org/10.5194/esd-9-757-2018.

https://doi.org/10.5194/egusphere-2026-6703
Preprint. Discussion started: 11 November 2026
© Author(s) 2026. CC BY 4.0 License.



National Water Information System (NWIS). (1998).

Penning-Rowsell, E. C., & Wilson, T. (2003). *The benefits of flood and coastal defence: techniques and data for 2003*. Middlesex University.

Rahman, M. S., Di, L., Yu, E., Lin, L., & Yu, Z. (2021). Remote sensing based rapid assessment of flood crop damage using novel disaster vegetation damage index (DVDI). *International Journal of Disaster Risk Science*, *12*, 90-110. https://doi.org/10.1007/s13753-020-00305-7.

Rahman, M. S., & Di, L. (2020). A systematic review on case studies of remote-sensing-based flood crop loss assessment. *Agriculture*, *10*(4), 131. https://doi.org/10.3390/agriculture10040131.

Reed, T., Mason, L. R., & Ekenga, C. C. (2020). Adapting to Climate Change in the Upper Mississippi River Basin: Exploring Stakeholder Perspectives on River System Management and Flood Risk Reduction. *Environmental Health Insights*, *14*, 1178630220984153. https://doi.org/10.1177/1178630220984153.

Reyes, J. J., & Elias, E. (2019). Spatio-temporal variation of crop loss in the United States from 2001 to 2016. *Environmental Research Letters*, *14*(7), 074017. https://doi.org/10.1088/1748-9326/ab1ac9.

Roesch-McNally, G. E., Arbuckle, J. G., & Tyndall, J. C. (2018). Barriers to implementing climate resilient agricultural strategies: The case of crop diversification in the U.S. Corn Belt. *Global Environmental Change*, *48*, 206–215. https://doi.org/10.1016/j.gloenvcha.2017.12.002

Scott, H. D., DeAngulo, J., Daniels, M. B., & Wood, L. S. (1989). Flood duration effects on soybean growth and yield. Agronomy Journal, 81(4), 631-636. https://doi.org/10.2134/agronj1989.00021962008100040016x.

Schechinger, A. (2022, January 27). *Crop losses from climate crisis cost billions of dollars in insurance payouts*. Environmental Working Group. https://www.ewg.org/research/crop-losses- climate-crisis-cost-billions-dollars-insurance-payouts.

Shan, J., Hussain, E., Kim, K., Biehl, L., & others. (2010). Flood mapping with satellite images and its web service. *Photogrammetric Engineering & Remote Sensing*, *76*(2), 102–105.

Shrestha, R., Di, L., Eugene, G. Y., Kang, L., SHAO, Y., & BAI, Y. (2017). Regression model to estimate flood impact on corn yield using MODIS NDVI and USDA cropland data layer. *Journal of Integrative Agriculture*, *16*(2), 398–407. https://doi.org/10.1016/S2095-3119(16)61502-2

Steele, C., Reyes, J., Elias, E., Aney, S., & Rango, A. (2018). Cascading impacts of climate change on southwestern US cropland agriculture. *Climatic Change*, *148*(3), 437–450. https://doi.org/10.1007/s10584-018-2220-4.

Suro, T. P., Roland, M. A., & Kiah, R. G. (2015). *Flooding in the Northeastern United States, 2011.*

Tate, E., Rahman, M. A., Emrich, C. T., & Sampson, C. C. (2021). Flood exposure and social vulnerability in the United States. *Natural Hazards*, *106*(1), 435–457. https://doi.org/10.1007/s11069-020-04470-2.

Tate, E., Strong, A., Kraus, T., & Xiong, H. Y. (2016). Flood recovery and property acquisition in Cedar Rapids, Iowa. *Natural Hazards*, *80*(3), 2055–2079. https://doi.org/10.1007/s11069-015-2060-8.

https://doi.org/10.5194/egusphere-2026-6703
Preprint. Discussion started: 11 November 2026
© Author(s) 2026. CC BY 4.0 License.



United States Department of Agriculture. (2010). *Field Crops: Usual Planting and Harvesting Dates*.

U.S. Geological Survey (USGS). (2019, May 10). *The StreamStats program*. Online at Https://Streamstats.Usgs.Gov/Ss/.

U.S. Geological Survey. (2022). *3D Elevation Program 1/3rd arc-second Digital Elevation Model (Published 2022-11-17)*.

Villa, P., & Gianinetto, M. (2006). Multispectral Transform and Spline Interpolation for Mapping Flood Damages. *2006 IEEE International Symposium on Geoscience and Remote Sensing*, 275–278. IEEE. https://doi.org/10.1109/IGARSS.2006.75.

Wang, X., Deng, Z., Zhang, W., Meng, Z., Chang, X., & Lv, M. (2017). Effect of waterlogging duration at different growth stages on the growth, yield and quality of cotton. *PloS one*, *12*(1), e0169029. https://doi.org/10.1371/journal.pone.0169029.

Ward, P. J., de Moel, H., & Aerts, J. C. J. H. (2011). How are flood risk estimates affected by the choice of return-periods? *Natural Hazards and Earth System Sciences*, *11*(12), 3181–3195. https://doi.org/10.5194/nhess-11-3181-2011.

Weisberger, D. A., McDaniel, M. D., Arbuckle, J. G., & Liebman, M. (2021). Farmer perspectives on benefits of and barriers to extended crop rotations in Iowa, USA. *Agricultural & Environmental Letters*, *6*(2), e20049. https://doi.org/10.1002/ael2.20049.

Wing, O. E., Bates, P. D., Sampson, C. C., Smith, A. M., Johnson, K. A., & Erickson, T. A. (2017). Validation of a 30 m resolution flood hazard model of the conterminous United States. *Water Resources Research*, *53*(9), 7968-7986. https://doi.org/10.1002/2017WR020917.

Wing, O. E. J., Bates, P. D., Smith, A. M., Sampson, C. C., Johnson, K. A., Fargione, J., & Morefield, P. (2018). Estimates of present and future flood risk in the conterminous United States. *Environmental Research Letters*, *13*(3), 34023. https://doi.org/10.1088/1748-9326/aaac65.

Wing, O. E. J., Lehman, W., Bates, P. D., Sampson, C. C., Quinn, N., Smith, A. M., Neal, J. C., Porter, J. R., & Kousky, C. (2022). Inequitable patterns of US flood risk in the Anthropocene. *Nature Climate Change*, *12*(2), 156–162. https://doi.org/10.1038/s41558-021-01265-6.

Yale Environment 360. (2022, January 28). *U.S. Drought- and Flood-Related Crop Insurance Payouts Have Tripled Since 1995*. Yale School of the Environment . https://e360.yale.edu/digest/u-s-drought-and-flood-related-crop-insurance-payouts-have-tripled- since-1995.

Yildirim, E., & Demir, I. (2022). Agricultural flood vulnerability assessment and risk quantification in Iowa. *Science of The Total Environment*, *826*, 154165. https://doi.org/10.1016/j.scitotenv.2022.154165.

Zarekarizi, M., Roop-Eckart, K. J., Sharma, S., & Keller, K. (2021). The FLOod Probability Interpolation Tool (FLOPIT): A Simple Tool to Improve Spatial Flood Probability Quantification and Communication. *Water*, *13*(5), 666. https://doi.org/10.3390/w13050666.

https://doi.org/10.5194/egusphere-2026-6703
Preprint. Discussion started: 11 November 2026
© Author(s) 2026. CC BY 4.0 License.



Zuzak, C., Mowrer, M., Goodenough, E., Burns, J., Ranalli, N., & Rozelle, J. (2022). The national risk index: establishing a nationwide baseline for natural hazard risk in the US. *Natural Hazards*, *114*(2), 2331-2355. https://doi.org/10.1007/s11069-022-05474-w.